



ATLAS NOTE

ATLAS-CONF-2012-149

November 10, 2012



Measurement of the top quark pair production cross section in the single-lepton channel with ATLAS in proton-proton collisions at 8 TeV using kinematic fits with b -tagging

The ATLAS Collaboration

Abstract

A measurement of the top quark pair ($t\bar{t}$) inclusive production cross section in pp collisions at a centre-of-mass energy of $\sqrt{s} = 8$ TeV is presented. Data were collected with the ATLAS detector at the CERN Large Hadron Collider. The analysis has been done in the lepton+jets final state in a dataset corresponding to an integrated luminosity of 5.8 fb^{-1} . A multivariate technique and b -jet identification were employed to separate the signal $t\bar{t}$ events from the various backgrounds. The inclusive $t\bar{t}$ production cross section is measured to be $\sigma_{t\bar{t}} = 241 \pm 2 \text{ (stat.)} \pm 31 \text{ (syst.)} \pm 9 \text{ (lumi.) pb}$ and is in good agreement with the theoretical prediction $\sigma_{t\bar{t}}^{\text{theor.}} = 238^{+22}_{-24} \text{ pb}$.

1 Introduction

The top quark is the heaviest fermion discovered so far. According to the Standard Model (SM), it has the largest Yukawa coupling with the Higgs boson. It may also couple to other heavy particles predicted by extensions of the SM. Additional processes beyond the SM can modify the top pair ($t\bar{t}$) production rate, therefore a measurement of the $t\bar{t}$ inclusive production cross section $\sigma_{t\bar{t}}$ may reveal the presence of new physics. It can also help to verify the state-of-the-art theoretical cross section calculations, and to better understand $t\bar{t}$ production as one of the primary backgrounds in many searches for physics beyond the SM.

The inclusive top quark pair production cross section has been measured by the ATLAS experiment in pp collisions at 7 TeV [1] and by CMS at 7 TeV [2] and 8 TeV [3]. All measurements have been found to be in good agreement with theoretical predictions for these energies. The predicted $t\bar{t}$ cross section for pp collisions at a centre-of-mass energy of $\sqrt{s} = 8$ TeV is $\sigma_{t\bar{t}}^{\text{theor.}} = 238^{+22}_{-24}$ pb for a top quark mass of 172.5 GeV. It has been calculated at approximate next-to-next-to-leading order (NNLO) in QCD with HATHOR 1.2 [4].

In the SM, the top quark decays to a W boson and a b -quark with a branching ratio close to 100%. The final event signature depends on the decay of the W boson. This analysis is based on final states where one of the W bosons decays leptonically into an electron or muon together with the corresponding neutrino, and the other decays hadronically. In this case the final state is characterized by the presence of a highly energetic and well isolated lepton, large missing transverse energy carried away by a neutrino, and at least four jets, two of which originate from b -quarks. Due to jet merging, the finite detector coverage, and jet reconstruction efficiencies it is possible to miss one of the four expected jets, leading to a three jet configuration in the final state. Therefore candidate events are selected by requiring at least three jets, with at least one of them identified as a b -jet. A multivariate likelihood method is used to provide signal-to-background discrimination. The number of $t\bar{t}$ events in data is determined from a fit to a distribution of the multivariate likelihood discriminant in data to a sum of signal and background distributions (“templates”). This number is then converted to the $t\bar{t}$ production cross section using the total integrated luminosity and the $t\bar{t}$ event selection efficiency. The latter is obtained using Monte Carlo (MC) simulation.

The note is organized as follows. The ATLAS detector and the data sample are described in Section 2. The MC samples for signal and backgrounds are listed in Section 3. Event selection and object definition are discussed in Section 4. Section 5 is devoted to the determination of the multijet background. The measurement strategy is outlined in Section 6. Section 7 lists the sources of systematic uncertainties considered in the analysis. Finally, the results of the analysis are summarized in Section 8.

2 ATLAS detector and data sample

The ATLAS detector [5] at the LHC covers nearly the entire solid angle around the collision point. It consists of an inner tracking detector surrounded by a thin superconducting solenoid, electromagnetic and hadronic calorimeters, and an external muon spectrometer incorporating three large superconducting toroid magnet assemblies.

The 8 TeV centre-of-mass energy data used in the analysis have been collected between April and June 2012 using single lepton (electron or muon) triggers. After data quality requirements, the amount of data used by the analysis corresponds to an integrated luminosity of 5.8 fb^{-1} . The average number of pp collisions per bunch crossing in the dataset is 19.3.

3 Signal and background simulation

The nominal MC sample used for the simulation of the $t\bar{t}$ events was produced using the MC@NLO v4.01 [6] event generator with the CT10 [7] parton distribution functions. The parton shower and the underlying event simulation were performed with HERWIG v6.520 [8] and JIMMY v4.31 [9], respectively, using the AUET2 tune [10]. Additional $t\bar{t}$ samples used to estimate various systematic effects were generated with POWHEG [11] interfaced to HERWIG/JIMMY, POWHEG interfaced to PYTHIA v6.4 [12], ACERMC generator v3.8 [13] interfaced to PYTHIA, and ALPGEN v2.13 [14] interfaced to HERWIG/JIMMY. Two samples of $t\bar{t}$ events produced at a centre-of-mass energy of $\sqrt{s} = 7$ TeV using the MC@NLO and ALPGEN generators were used for evaluation of the systematic uncertainty due to MC modelling of the signal. Both samples were reweighted using PDF rescaling to match the $t\bar{t}$ production at $\sqrt{s} = 8$ TeV.

The backgrounds are expected to originate from vector boson production with associated jets (W +jets and Z/γ^* +jets), single top, diboson (WW , WZ , ZZ), and multijet production. All backgrounds except that from multijet production in the μ +jets channel were simulated with MC. The dominant background (vector boson production with associated jets) was simulated using ALPGEN interfaced to HERWIG/JIMMY. The W +jets normalization was derived from a fit to the data as explained in Section 8. The contribution from single top quark production was simulated with MC@NLO interfaced to HERWIG/JIMMY for the s - and Wt -channels, and with ACERMC interfaced to PYTHIA for the t -channel, and normalized to approximate NNLO theoretical cross sections [15–17]. Finally, diboson production was simulated with HERWIG.

All generated events were passed through the full ATLAS detector simulation [18] based on GEANT4 [19] and then processed with the same reconstruction chain as the data. MC events were overlaid with additional minimum bias events generated with PYTHIA to simulate the effect of additional proton-proton interactions. The multijet background was estimated using the methods described in Section 5.

4 Event selection

The present analysis relies on the measurement of jets, electrons, muons and the magnitude of the missing transverse energy E_T^{miss} . Jets were reconstructed using the anti- k_t algorithm [20] with a distance parameter $R = 0.4$. Jets from additional proton-proton interactions were suppressed by requiring the jet vertex fraction (JVF) to be larger than 0.5. The JVF value is defined using tracks matched to the jet as the ratio of the scalar sum of transverse momenta of tracks associated to the primary vertex to that of all tracks. Jets were b -tagged using the MV1 [21] algorithm at 70% b -tagging efficiency operating point. Data-to-MC corrections derived for this tagger were used to compensate the differences between the tagger algorithm performance on data and MC. For that purpose, the results obtained with 7 TeV data [21–24] have been updated with 8 TeV data.

Electrons were identified as energy clusters in the electromagnetic calorimeter matched to a reconstructed track in the inner detector and fulfilling additional isolation requirements in both the calorimeter and the inner detector. Electrons were required to have transverse energy $E_T > 40$ GeV and pseudorapidity in the range $|\eta| < 2.47$ excluding the region $1.37 < |\eta| < 1.52$. Muons were reconstructed using information from the muon spectrometer and the inner detector. They were required to have transverse momentum $p_T > 40$ GeV and pseudorapidity $|\eta| < 2.5$. As for electrons, isolation criteria were imposed on muons in both the calorimeter and the inner detector. Both electrons and muons in MC were corrected to reflect the performance observed in the data. The missing transverse energy E_T^{miss} was calculated from the vectorial energy sum of all topological clusters in the calorimeter and transverse momenta of reconstructed muons. More details on the reconstruction of objects can be found in [25].

The events were selected using the following criteria:

- the appropriate single-electron or single-muon trigger fired;
- a primary vertex reconstructed from at least five tracks;
- at least three jets with $p_T > 25$ GeV and $|\eta| < 2.5$;
- a reconstructed electron with $E_T > 40$ GeV or muon of $p_T > 40$ GeV matching the corresponding high level trigger object;
- no second lepton (reconstructed electron with $E_T > 25$ GeV or muon with $p_T > 25$ GeV);
- in the e +jets channel: $E_T^{\text{miss}} > 30$ GeV and the transverse mass of the W boson¹ $m_T(W) > 30$ GeV;
- in the μ +jets channel: $E_T^{\text{miss}} > 20$ GeV and $m_T(W) + E_T^{\text{miss}} > 60$ GeV;
- at least one selected jet in the event must be identified as a b -jet.

Compared to the previous analyses [1, 26] the electron E_T and muon p_T cuts were increased to control the multijet background.

The number of events observed in data and expected yield of events based on simulation are summarized in Table 1.

Table 1: The numbers of expected events from signal and backgrounds and numbers of events observed in data. The multijet uncertainty is assumed to be 50%. All other uncertainties are derived using theoretical cross section uncertainties only.

	$e + \geq 3$ jets	$\mu + \geq 3$ jets
$t\bar{t}$	31000^{+2900}_{-3100}	44000 ± 4000
W +jets	5700 ± 2400	9000 ± 4000
Multijet	1900 ± 900	1100 ± 500
Z +jets	1400 ± 600	1200 ± 500
Single top	3260 ± 160	4610 ± 230
Dibosons	115 ± 6	158 ± 8
Total Expected	43000 ± 4000	61000 ± 6000
Data	40794	58872

5 Multijet background evaluation

Events with vector bosons in the final state, as selected by single lepton triggers, are characterized by the presence of high- p_T isolated leptons. The processes that give rise to “fake” leptons (either non-isolated leptons or objects mimicking isolated leptons) include semileptonic b -quark decays, photon conversions, decays of long-lived particles that produce an electron or a muon in the decay chain, or mis-identification of jets as electrons.

Two different methods were employed in this analysis for the fake lepton background evaluation. The Matrix Method (MM) [27] was used to obtain the estimation of the fake lepton background in the μ +jets channel. In this method, the probability for a high- p_T signal lepton to pass the standard event selection

¹The transverse mass is defined as $m_T(W) = \sqrt{2p_T^\ell p_T^\nu (1 - \cos(\phi^\ell - \phi^\nu))}$, where p_T is the transverse momentum, ϕ is the azimuthal angle, and ℓ and ν refer to the charged lepton and the neutrino, respectively.

criteria was derived with data in the high $E_T^{\text{miss}} > 80$ GeV region free of fake lepton contamination. The probability for a fake lepton to pass the same criteria was obtained from the low $E_T^{\text{miss}} < 20$ GeV region after the subtraction of the contribution from the W/Z decays as predicted by MC. In the $e+\text{jets}$ channel, the Jet-electron method [25] using a dijet sample simulated with PYTHIA was applied. The shape of the fake lepton background was determined by selecting events with similar kinematics to the signal selection, with jets mimicking electrons. The background from photon conversions was suppressed by demanding at least four tracks to be associated with the jet. The estimation of the multijet background obtained with the Jet-electron method was performed by fitting the E_T^{miss} distribution.

6 Analysis method

The analysis strategy is as follows. The number of $t\bar{t}$ events is obtained from the data using a likelihood discriminant template fit. The likelihood discriminant function is constructed using the projective likelihood method defined in the TMVA package [28]. The likelihood discriminant for event i is defined as the ratio of the signal likelihood L_i^s to the sum of signal and background likelihoods ($L_i^s + L_i^b$):

$$D_i = \frac{L_i^s}{(L_i^s + L_i^b)} \quad (1)$$

The signal and background likelihoods are defined as products of the corresponding probability density functions of each kinematic variable used in the likelihood. For the likelihood construction, the $t\bar{t}$ and $W+\text{jets}$ events are considered as signal and background, respectively. After the likelihood discriminant function is constructed, binned distributions (templates) are made for the $t\bar{t}$ signal and each of the backgrounds.

The variables used in the likelihood are lepton pseudorapidity η_l and the transformed event aplanarity $A' = \exp(-8A)$, where the (regular) aplanarity A is defined as $A = \frac{3}{2}\lambda_3$, λ_3 being the smallest eigenvalue of the normalized momentum tensor calculated using the momenta of all jets and the lepton. The $A \rightarrow A'$ transformation is done in order to increase the separation power of the aplanarity distribution as discussed in Ref. [29].

The number of $t\bar{t}$ events in each channel j is obtained by minimizing the log-likelihood function

$$\sum_i v_{ij} - n_{ij} + n_{ij} \ln n_{ij} - n_{ij} \ln v_{ij}, \quad (2)$$

where the sum is taken over all template bins i . The observed number of events is n_{ij} , while v_{ij} is the expected number of events. The latter is defined as

$$v_{ij} = p^{t\bar{t}} s_{ij} + p_j^W b_{ij} + m_{ij}, \quad (3)$$

where s_{ij} , b_{ij} , and m_{ij} are the predicted numbers of events for the $t\bar{t}$ signal, the $W+\text{jets}$, and other backgrounds ($Z+\text{jets}$, single top, dibosons, and multijet), respectively, and $p^{t\bar{t}}$, p_j^W are the parameters of the fit (equal to 1 for a cross section equal to the MC expectation). The resulting value of the fit parameter $p^{t\bar{t}}$ is used to extract the number of $t\bar{t}$ events in the data.

The combination of the $e+\text{jets}$ and $\mu+\text{jets}$ channels is done by minimizing the sum of (2) over both channels. The contributions from $W+\text{jets}$ are fitted separately in the $e+\text{jets}$ and $\mu+\text{jets}$ channels. This is done because the $W+\text{jets}$ fraction variation can absorb uncertainties in other backgrounds, notably in $Z+\text{jets}$ (see further discussion in Section 7).

The likelihood discriminant distribution in data fitted to the sum of the signal and background templates is shown in Fig. 1. An example of the comparison between data and MC for the likelihood variables

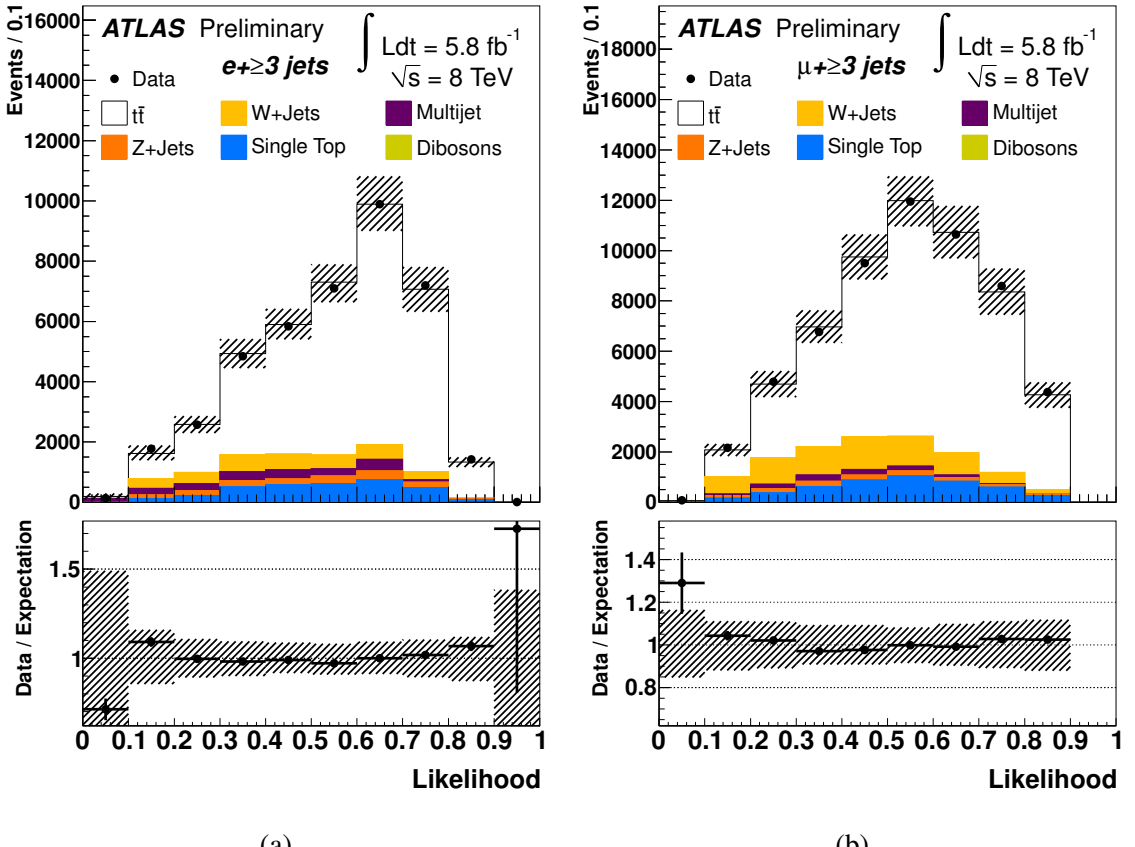


Figure 1: Fit to the likelihood discriminant distribution $D(\eta_l, A')$ in data in the e +jets (a) and μ +jets (b) channels. The hatched bands display the combined expected statistical and systematic uncertainty.

after the fit is shown in Fig. 2. Figures 3 and 4 show distributions of basic kinematic quantities after the fit in both channels.

The $t\bar{t}$ production cross section is calculated as

$$\sigma_{t\bar{t}} = \frac{N_{t\bar{t}}}{\mathcal{L} \times BR \times \varepsilon_{\text{sig}}}, \quad (4)$$

where \mathcal{L} is the integrated luminosity, BR is the combined branching ratio for dileptonic and semileptonic $t\bar{t}$ decays, and ε_{sig} is the product of the signal acceptance and efficiency calculated on a $t\bar{t}$ sample without fully-hadronic decays.

The fitted numbers $N_{t\bar{t}}$ of $t\bar{t}$ events and the corresponding cross sections are shown in Table 2. The quoted statistical uncertainties are evaluated from the fit. The fitted W +jets scale factors p_j^W are found to be 0.54 ± 0.05 (stat.) in the e +jets channel and 0.73 ± 0.04 (stat.) in the μ +jets channel. The correlation coefficient between the $t\bar{t}$ and W +jets fractions is found to be -0.7 for both channels.

7 Systematic uncertainties

The systematic uncertainties relevant to this analysis fall into several categories. The instrumental systematic uncertainties are related to the reconstruction of jets and E_T^{miss} (jet energy scale, jet energy resolution, jet reconstruction efficiency, soft jet related uncertainties in E_T^{miss} calculations), and leptons

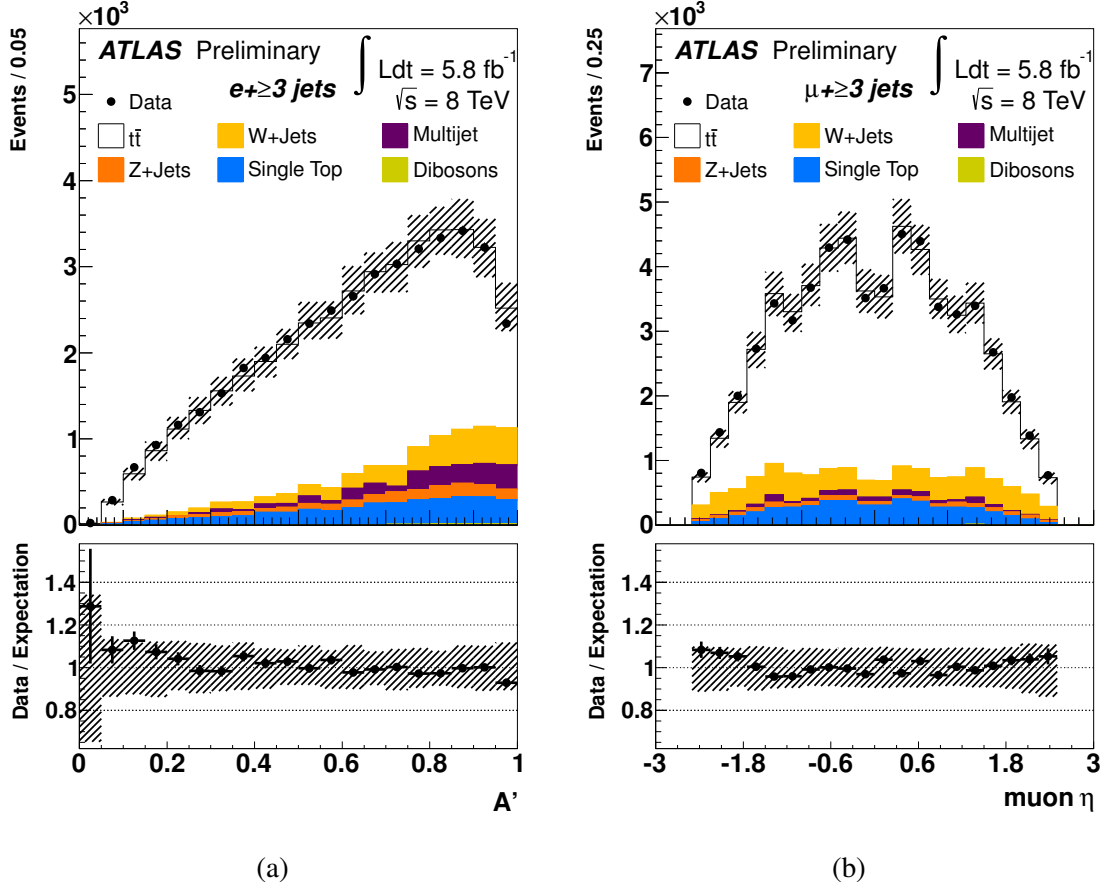


Figure 2: Transformed aplanarity A' distribution in the e +jets channel (a) and muon pseudorapidity η distribution in the μ +jets channel (b). The distributions in the data (dots) are compared to the model expectations, which include both signal and background processes. The hatched bands display the combined expected statistical and systematic uncertainty.

Table 2: Number of $t\bar{t}$ events and corresponding cross sections obtained from the likelihood fit to data together with their statistical uncertainties.

Channel	$N_{t\bar{t}}$	$\sigma_{t\bar{t}}$ (pb)
$e+\geq 3$ jets	31050 ± 350	239 ± 3
$\mu+\geq 3$ jets	45000 ± 400	242 ± 2
$l+\geq 3$ jets	76000 ± 500	241 ± 2

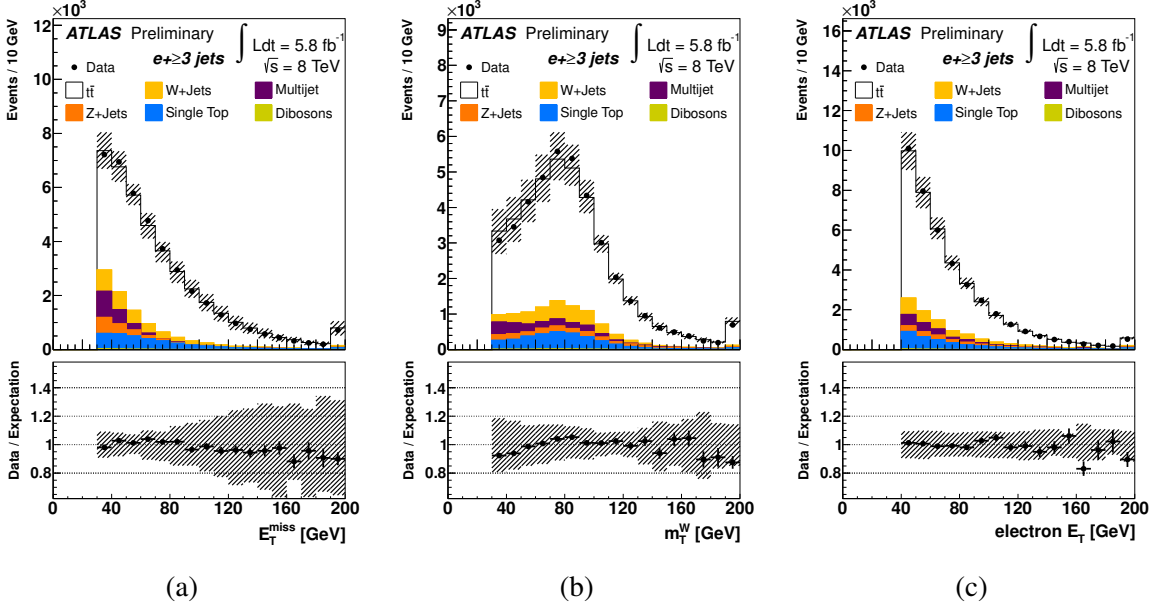


Figure 3: Missing transverse energy (a), transverse W mass (b), and electron E_T (c) distributions in the $e+jets$ channel. The distributions in the data (dots) are compared to the model expectations, which include both signal and background processes. The hatched bands display the combined expected statistical and systematic uncertainty.

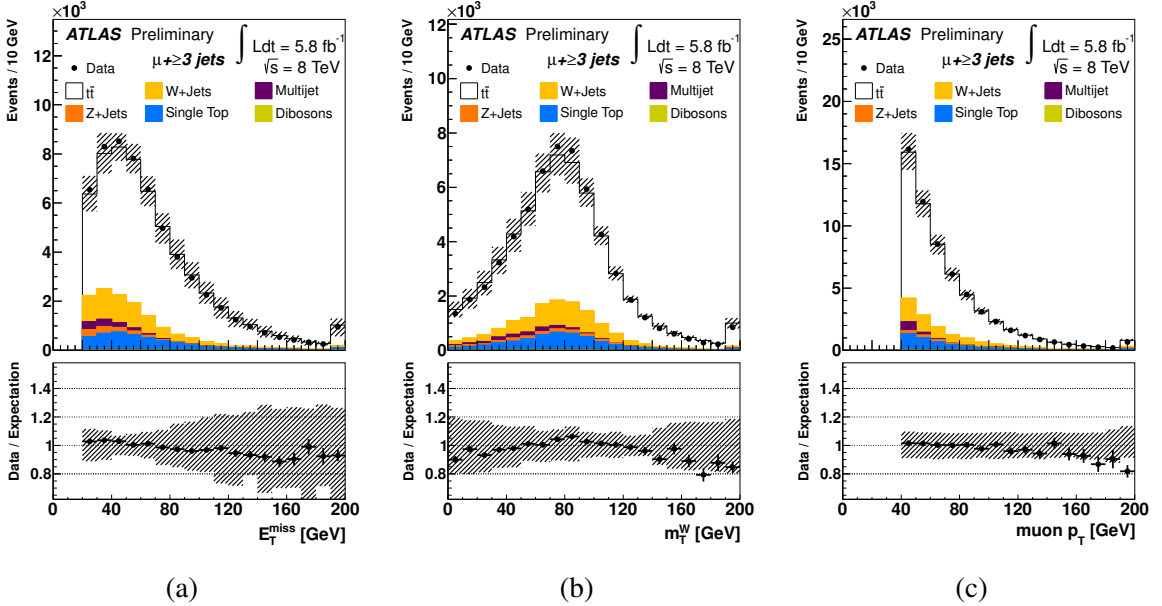


Figure 4: Missing transverse energy (a), transverse W mass (b), and muon p_T (c) distributions in the $\mu+jets$ channel. The distributions in the data (dots) are compared to the model expectations, which include both signal and background processes. The hatched bands display the combined expected statistical and systematic uncertainty.

(momentum/energy scale and resolution, trigger efficiency, reconstruction and lepton identification efficiency), as well as the b -tagging performance uncertainty. All of these uncertainties are evaluated by performing ensemble tests using modified likelihood templates for signal and background. The dominant instrumental systematic uncertainty (6%) is due to the jet energy scale, and here mostly due to its impact on the signal reconstruction efficiency.

For the multijet contribution, the variation of results due to scaling of the background up and down by 50%, as well as the difference between results obtained using the Matrix Method and the Jet-electron model, were used as a systematic uncertainty. Because of the low level of multijet background in the selected sample the systematic uncertainty on the cross section $\sigma_{t\bar{t}}$ due to multijet modelling is small (about 1%).

As discussed in Section 6, the contributions from W +jets are fitted separately in the e +jets and μ +jets channels to allow for absorption of uncertainties in other backgrounds. To verify the fitting procedure, W +jets and Z +jets were merged into a single template and the combined fit was performed with the W/Z +jets cross section forced to be the same in both channels. The difference in the $t\bar{t}$ cross section obtained by the two methods is small (0.2%).

The systematic uncertainty related to the modelling of W +jets, which results in a variation of likelihood template shapes, is found to be small (<1%). The systematic uncertainty due to single top, diboson, and Z +jets production is evaluated by varying their cross sections [27]. The effect on the $t\bar{t}$ cross section is also small (about 1%).

The uncertainty due to the modelling of Initial/Final State Radiation (ISR/FSR) is estimated using $t\bar{t}$ events produced with the ACERMC generator interfaced with PYTHIA, where the parameters controlling ISR/FSR were varied in a range suggested by the data in the rapidity gap analysis [30, 31]. The resulting $\sigma_{t\bar{t}}$ uncertainty is 4%. The systematic uncertainty due to MC modelling of the $t\bar{t}$ production process is estimated by comparing results obtained with MC@NLO, POWHEG, and ALPGEN signal samples. This uncertainty is found to be 6%. In addition, there are uncertainties due to parton distribution functions (PDF) 6% and the choice of the parton shower model, the latter being estimated by comparing results obtained with POWHEG interfaced to PYTHIA and HERWIG (6%). Finally, the luminosity uncertainty, measured using techniques similar to those described in [32, 33], is 3.6%. This uncertainty is quoted separately.

The systematic uncertainties on the inclusive $t\bar{t}$ cross section measurement are summarized in Table 3. The uncertainties due to ISR/FSR, MC generator modelling, PDF, and parton shower model are combined in a single category named “MC modelling of the signal.”

Table 3: Systematic uncertainties (%) on the inclusive $t\bar{t}$ cross section measurement in the lepton+jets channel.

Source	$e+ \geq 3$ jets	$\mu+ \geq 3$ jets	combined
Jet/MET reconstruction, calibration	6.7, -6.3	5.4, -4.6	5.9, -5.2
Lepton trigger, identification and reconstruction	2.4, -2.7	4.7, -4.2	2.7, -2.8
Background normalization and composition	1.9, -2.2	1.6, -1.5	1.8, -1.9
b -tagging efficiency	1.7, -1.3	1.9, -1.1	1.8, -1.2
MC modelling of the signal	± 12	± 11	± 11
Total	± 14	± 13	± 13

The $t\bar{t}$ production cross section is determined under the assumption of a fixed top quark mass $m_{\text{top}} = 172.5$ GeV. Using the $t\bar{t}$ MC samples generated with $m_{\text{top}} = 170$ and 175 GeV, it is observed that the result varies by $\pm 1\%$ when m_{top} changes by ± 2.5 GeV. This variation is not included in the systematic

uncertainty.

8 Summary of results

A measurement of the inclusive $t\bar{t}$ production cross section in pp collisions at $\sqrt{s} = 8$ TeV using the ATLAS detector at the Large Hadron Collider has been performed using a data set corresponding to an integrated luminosity of 5.8 fb^{-1} . The cross section is found to be

$$\sigma_{t\bar{t}} = 241 \pm 2 \text{ (stat.)} \pm 31 \text{ (syst.)} \pm 9 \text{ (lumi.) pb.}$$

This result is in good agreement with the current theoretical prediction $\sigma_{t\bar{t}}^{\text{theor.}} = 238^{+22}_{-24} \text{ pb}$ for a top quark mass of 172.5 GeV as obtained from approximate NNLO QCD calculations with HATHOR 1.2 [4].

References

- [1] ATLAS Collaboration, *Measurement of the $t\bar{t}$ production cross-section in pp collisions at $\sqrt{s} = 7$ TeV using kinematic information of lepton+jets events*, ATLAS-CONF-2011-121, 2011.
- [2] CMS Collaboration, *Measurement of the Top-antitop Production Cross Section in pp Collisions at $\sqrt{s} = 7$ TeV using the Kinematic Properties of Events with Leptons and Jets*, arXiv:1106.0902 [hep-ex], Eur.Phys.J. **C71** (2011), 1721.
- [3] CMS Collaboration, *Top pair cross section in $e\mu+jets$ at 8 TeV*, CMS-PAS-TOP-12-006, 2012.
- [4] M. Aliev et al., *HATHOR - Hadronic Top and Heavy quarks cross section calculator*, arXiv:1007:1327 [hep-ph], Comput. Phys. Commun. **182** (2011), 1034–1046.
- [5] ATLAS Collaboration, *ATLAS experiment at the CERN Large Hadron Collider*, JINST **3** (2008), S08003.
- [6] S. Frixione, B. Webber, et al., *Matching NLO QCD computations and parton shower simulations*, arXiv:hep-ph/0204244, JHEP **029** (2002), 0206.
- [7] H.-L. Lai et al., *New parton distributions for collider physics*, arXiv:1007.2241 [hep-ph], Phys. Rev. **D82** (2010), 074024.
- [8] G. Corcella et al., *HERWIG 6: An Event generator for hadron emission reactions with interfering gluons (including supersymmetric processes)*, arXiv:hep-ph/0011363, JHEP **010** (2001), 0101.
- [9] J. M. Butterworth, J. R. Forshaw, and M. H. Seymour, *Multiparton interactions in photoproduction at HERA*, arXiv:hep-ph/9601371, Z. Phys. **C72** (1996), 637–646.
- [10] ATLAS Collaboration, *New ATLAS event generator tunes to 2010 data*, ATL-PHYS-PUB-2011-008, 2010.
- [11] S. Frixione, P. Nason and C. Oleari, *Matching NLO QCD computations with Parton Shower simulations: the POWHEG method*, arXiv:0709.2092 [hep-ph], JHEP **0711** (2007), 070.
- [12] T. Sjostrand and S. Mrenna and P.Z. Skands, *PYTHIA 6.4 Physics and Manual*, arXiv:hep-ph/0603175, JHEP **05** (2006), 026.
- [13] B.P. Kersevan and E. Richter-Wąs, *The Monte Carlo event generator AcerMC version 2.0 with interfaces to PYTHIA 6.2 and HERWIG 6.5*, arXiv:hep-ph/0405247, (2004).
- [14] M.L. Mangano et al., *ALPGEN, a generator for hard multiparton processes in hadronic collisions*, arXiv:hep-ex/0206293, JHEP **0307** (2003), 001.
- [15] N. Kidonakis, *Next-to-next-to-leading-order collinear and soft gluon corrections for t -channel single top quark production*, arXiv:1103.2792 [hep-ph], Phys. Rev. **D83** (2011), 091503.
- [16] N. Kidonakis, *NNLL resummation for s -channel single top quark production*, arXiv:1001.5034 [hep-ph], Phys. Rev. **D81** (2010), 054028.
- [17] N. Kidonakis, *Two-loop soft anomalous dimensions for single top quark associated production with a W - or H -*, arXiv:1005.4451 [hep-ph], Phys. Rev. **D82** (2010), 054018.
- [18] ATLAS Collaboration, *The ATLAS Simulation Infrastructure*, arXiv:1005.4568 [physics.ins-det], Eur. Phys. J. **C70** (2010), 823–874.

- [19] S. Agostinelli et al. (GEANT4 Collaboration), *GEANT4 - A Simulation Toolkit*, Nucl. Instr. and Meth. **A506** (2003), 250.
- [20] M. Cacciari, G. P. Salam, and G. Soyez, *The Anti- $k(t)$ jet clustering algorithm*, arXiv:0802.1189 [hep-ph], JHEP **0804** (2008), 063.
- [21] ATLAS Collaboration, *Measurement of the b-tag Efficiency in a Sample of Jets Containing Muons with 5 fb^{-1} of Data from the ATLAS Detector*, ATLAS-CONF-2012-043, 2012.
- [22] ATLAS Collaboration, *Measuring the b-tag efficiency in a ttbar sample with 4.7 fb^{-1} of data from the ATLAS detector*, ATLAS-CONF-2012-097, 2012.
- [23] ATLAS Collaboration, *b-jet tagging calibration on c-jets containing D^{*+} mesons*, ATLAS-CONF-2012-039, 2012.
- [24] ATLAS Collaboration, *Measurement of the Mistag Rate with 5 fb^{-1} of Data Collected by the ATLAS Detector*, ATLAS-CONF-2012-040, 2012.
- [25] ATLAS Collaboration, *Measurement of t-Channel Single Top-Quark Production in pp Collisions at $\sqrt{s} = 8\text{ TeV}$ using Neural Networks*, ATLAS-CONF-2012-132, 2012.
- [26] ATLAS Collaboration, *Measurement of the top quark pair production cross section with ATLAS in pp collisions at $\sqrt{s} = 7\text{ TeV}$ in the single-lepton channel using semileptonic b-decays*, ATLAS-CONF-2012-131, 2012.
- [27] ATLAS Collaboration, *Measurement of the top quark-pair production cross section with ATLAS in pp collisions at $\sqrt{s} = 7\text{ TeV}$* , arXiv:1012.1792 [hep-ex], Eur. Phys. J. **C71** (2011), 1577.
- [28] A. Höcker et al., *TMVA: Toolkit for multivariate data analysis*, arXiv:physics/0703039, PoS **ACAT** (2007), 040.
- [29] ATLAS Collaboration, *Measurement of the top quark pair production cross-section with ATLAS in the single lepton channel*, arXiv:1201.1889 [hep-ex], Phys. Lett. **B711** (2012), 244–263.
- [30] ATLAS Collaboration, *Measurement of dijet production with a veto on additional central jet activity in pp collisions at $\sqrt{s} = 7\text{ TeV}$ using the ATLAS detector*, arXiv:1107.1641 [hep-ex], JHEP 09 (2011), 053.
- [31] ATLAS Collaboration, *Measurement of $t\bar{t}$ production with a veto on additional central jet activity in pp collisions at $\sqrt{s} = 7\text{ TeV}$ using the ATLAS detector*, arXiv:1203.5015 [hep-ex], Eur. Phys. J. **C72** (2012), 2043.
- [32] ATLAS Collaboration, *Luminosity determination in pp collisions at $\sqrt{s} = 7\text{ TeV}$ using the ATLAS Detector at the LHC*, arXiv:1101.2185 [hep-ex], Eur. Phys. J. **C71** (2011), 1630.
- [33] ATLAS Collaboration, *Luminosity determination in pp collisions at $\sqrt{s} = 7\text{ TeV}$ using the ATLAS Detector in 2011*, ATLAS-CONF-2011-116, 2011.